Off-design performance modeling results for a supercritical CO₂ waste heat recovery power system

Steven A. Wright

SuperCritical Technologies, Inc.
5747 Imperial Way SW, Bremerton, WA 98312
swright@supercritical.tech

Chief Scientist: *Global leader in SuperCritical Power Systems Retired Sandia National Labs, PhD Nuclear Engineering, UW*

Chal S. Davidson

SuperCritical Technologies, Inc.
5747 Imperial Way SW, Bremerton, WA 98312
cdavidson@supercritical.tech

Chief Technology Officer: *Naval propulsion and SuperCritical CO2 expert Lockheed Martin, Knolls Atomic Power Labs, Bechtel, TerraPower, Intellectual Ventures. B.S. and M.S. in Nuclear Engineering, UW MBA*

Craig Husa

SuperCritical Technologies, Inc.
5747 Imperial Way SW, Bremerton, WA 98312
chusa@supercritical.tech

CEO:, *As founder or CEO, grew & sold four companies for large returns, Most recently 3TIER. General Software, CourtLink, Nuclear-trained Naval Officer. US Naval Academy, Harvard MBA*

ABSTRACT

The results of off-design performance models for a sCO₂ (supercritical CO₂) bottoming cycle are presented. The sCO₂ power cycle uses split flow with preheating [1] to make effective use of the available exhaust gas heat from a 15 MWe Titan 130 gas turbine. Approximately 80-82% of the exhaust gas heat is transferred to the sCO₂. The sCO₂ power cycle uses dry cooling, and the plant produces nominally 5 MWe. A low-pressure boost compressor [2] is included in the power plant to provide for startup and load following. Additional controls include the cooling air flow rate, the total pressure ratio, and split-flow control fraction. These controls are used to mitigate the effects of increases in ambient heat rejection temperature. CO₂ pressure control will be used to take advantage of lower ambient temperature variations when condensation can occur in the CO₂ cooling system. This allows the power system to switch from operating in the supercritical mode to operating in the transcritical mode. The main

features that are used for control consist of the variable speed boost compressor, CO_2 pressure regulation, heat rejection air flow (fan speed), plus valves to control the CO_2 flow split, compressor recirculation, and/or exhaust gas flow through the CO_2 heaters that is implemented via a stack bypass valve. In addition, turn-down of the Titan 130 is allowed. Examples of steady state off-design performance will be provided in the presentation to illustrate the expected behavior of the s CO_2 power plant.

The off-design code uses physical models based on vendor quotes for all components including the turbines and compressors, heat exchangers and other components. The turbomachinery operating models are based on simplified non-dimensional models for the compressors and turbines that were used in the Sandia National Lab sCO₂ research experiments [3]. The Engineering Equation Solver EES64 is used for the off-design models and for the CO_2 equation of state [4].

Nomenclature					
A	heat transfer area	LP	Low Pressure Leg	$\dot{V}$	volumetric flow rate
C	Degrees C	LMDT	log-mean-delta-temperature		
c	spouting velocity	MW	Megawatt	*Subscripts*	
CC	Combined Cycle	MWe	Megawatt-electric	*ad*	*Adiabatic*
Chlr	Chiller	N	shaft speed rps	*cg*	*combustion gas*
CO₂	Carbon dioxide	Ns	Specific speed	*e*	*Electric*
comp	Component or Compressor	NTU	Number of Heat Trans Units	*Gen*	*at Generator term.*
		p	pressure Q_ad Adiabatic head coef.	*th*	*Thermal*
dH	change in enthalpy			*op*	*operating (speed)*
dH_ad	adiabatic enthalpy change	Pwr	Power	*tot*	*Total (sum over items)*
Duct	Mass in Ducting	PreHtr	Preheater (Hx)		
Ds	Specific diameter	PrimHx	Primary Heat Exchanger	*WF*	*Working Fluid*
Eff	Efficiency	Q	heat transfer	*1…11*	*Node Location*
Effect	Effectiveness of Hx	Recup	recuperator		
K	Degrees K	rpm	revolutions per minute	*Acronyms*	
h	enthalpy	rps	revolutions per second	HRU	Heat Recovery Unit
HP	high pressure (leg)	s	second	WHR	Waste Heat Recovery
Hrs	hours	sCO₂	Supercritical CO₂	MC1	Main Compressor 1 (Boost)
htc	heat transfer coefficient	T	temperature		
HT	high temperature	turb	turbine	MC2	Main Compressor 2 (Feed)
Hx	heat exchanger	U	universal heat transfer coef.		
kg	kilograms (kg or Kg)	u	tip speed	ORC	Organic Rankine Cycle
kPa	kilopascals				
kW	kilowatt				

1. Introduction

Supercritical Technologies Inc. is developing a 5 MWe class sCO₂ power system for use as a bottoming cycle for medium sized gas turbines. Figure 1A shows the steady-state off-design process flow model results for the sCO₂ power plant operating at the design point. The sCO₂ Waste Heat Recovery (WHR) plant is connected to a Titan 130 gas turbine that produces about 15 MWe at the generator terminals while the WHR sCO2 plant produces nominally 5 MWe at the generator terminals for a total power of nominally 20 MWe. The net combined cycle efficiency at the generator terminals is expected to be near 47%-48% depending on operating conditions. The power plant uses an air-cooled heat exchanger and thus, no water is needed. Figure 2 provides an engineering drawing of an early conceptual design of the combined cycle power plant. A biomass version of the sCO₂ plant is also being developed.

The business model for these plants is focused on distributed power, and priority power applications that have both growth potential and volume sales opportunities.

1.1 Split Flow with Preheating Power Cycle

The sCO_2 WHR cycle uses a "Split Flow with Preheating" power cycle to convert the waste heat to electrical power. This power cycle is a modification of the simple recuperated Brayton cycle and was first described by Campanari, Lozza, and Macchi[1]. It was developed to make effective use of the available exhaust gas heat and is often used in Organic Rankine cycle power systems[2]. The Split Flow with preheating power cycle has two major advantages for sCO_2 power systems. First it helps avoid a thermal pinch in the recuperator because only a fraction of the total mass flow is through the high-pressure leg, which has the highest heat capacity. Second the preheating allows the power plant to make effective use of the sensible heat from the gas turbine exhaust by using the preheater sCO_2 flow to lower the combustion gas exit temperature to a value that is only a little above the sCO_2 compressor exit temperature (70-80 C) as illustrated in Figure 1B. Typically, it is desired to reduce the combustion gas exit temperature to 90 C-120 C to avoid condensation in the stack. The performance and economic benefits of this and other waste heat recovery sCO_2 power conversion cycles are described in Wright and Scammel[7].

1.2 Titan 130 Gas Turbine

The Titan 130 gas turbine gas exhaust contains approximately 25.26 MW of thermal heat at 512 C and a flow rate of 47.13 kg/s [5,6] with a reference temperature of 20.4 C. The gas turbine produces nominally 15 MWe at the generator terminals at an efficiency of 35.2%. Approximately 80% of the exhaust gas heat is transferred to the CO_2 in the primary and preheater heat exchangers. Approximately 25% of this heat is then converted to electricity in the sCO_2 power cycle.

1.3 sCO_2 WHR cycle

The proposed sCO_2 WHR power cycle uses air cooled heat exchangers, and the plant produces 4.5 MWe at the generator terminals. Figure 2 shows an early conceptual 3D illustration of the combined cycle plant. The sCO_2 bottoming cycle consists of four main modules including the Heat Recovery Unit (HRU), the integrally geared turbo-compressor-machinery including the recuperator, the air-cooled heat exchangers, and an inventory tank. The Heat Recovery Unit is located between the Titan 130 and the exhaust stack. The integrally geared turbomachinery connects the shaft of the motor-generator to a bull gear which spins one or more pinions containing the feed compressor (MC2) and the main turbine. The turbomachinery is connected via piping to the recuperator. The main piping lengths connect the turbo-compressors and recuperator to the HRU and also to the CO_2 air cooled chiller. Note that the turbomachinery is very small and has dimensions that are only a little larger than the piping, so it is difficult to see in the figure.

In the proposed design, a low-pressure boost compressor[2] is placed in series with the main feed compressor (MC1 in Figure 1, not shown in Figure 2). This "boost compressor" was included in the power cycle to provide for startup and to improve operations during off-design conditions. This power cycle was tested by Caterpillar in a ORC power plant as described by Montgomery[2].

Figure 1 A: **Off Design Performance for a sCO2 WHR Bottoming Cycle with Titan 130 Gas Turbine**

$Pwr_{1stLaw} = 5056$ [kW] $Eff_{th} = 0.2519$ $Pwr_{GenNet} = 4573$ [kW] $Eff_{Net} = 0.2278$ $Eff_{CC} = 0.4694$ $Eff_{WHR} = 0.7948$

Boost Compressor

Feed Compressor

Generator   Turbine

$T_7 = 347.8$ [C]
$p_7 = 19622$ [kPa]

$Pwr_{op,Turb} = 7574$ [kW]
$Eff_{op,Turb} = 0.8595$
$RPM_{op,Turb} = 18600$ [1/min]

$Pwr_{op.MC2} = 1626$ [kW]
$Eff_{op,MC2} = 0.8122$
$RPS_{op,MC2} = 310$ [1/s]

$T_3 = 75.12$ [C]
$p_3 = 19787$ [kPa]

$T_2 = 51.29$ [C]
$p_2 = 11696$ [kPa]
$mdot_2 = 96.12$ [kg/s]

$Pwr_{op,MC1} = 891.8$ [kW]
$Eff_{op,MC1} = 0.8141$
$RPM_{op,MC1} = 11400$ [1/min]
$RPS_{op,MC1} = 190$ [1/s]

$T_1 = 34.58$ [C]
$p_1 = 8000$ [kPa]

$P_{airIn} = 99.71$ [kPa]
$T_{airIn} = 20.05$ [C]

$Q_{chlr} = 15020$ [kW]

SCO2 Chiller

$mdot_{Air,Chlr} = 545.6$ [kg/s]

$T_{Air,Chlr,Out} = 47.43$ [C]

$LMDT_{Chlr} = 23.12$ [C]
$Pwr_{Fan,Chlr} = 157.9$ [kW]

$mdot_8 = 96.12$ [kg/s] $T_8 = 261$ [C]

$p_8 = 8157$ [kPa]

$mdot_4 = 69.2$ [kg/s]
$LMDT_{HTrecup} = 9.95$ [C] $T_4 = 75.12$ [C]
$eff_{HTrecup} = 0.9472$
$p_4 = 19787$ [kPa]

$T_5 = 247.2$ [C]
$p_5 = 19725$ [kPa]

$f_{split} = 0.72$

$mdot_5 = 69.2$ [kg/s]

$T_9 = 81.99$ [C]
$p_9 = 8023$ [kPa]

$mdot_9 = 96.12$ [kg/s]

Recuperator

$mdot_7 = 96.12$ [kg/s]

$T_{11} = 245.1$ [C]

$p_{11} = 19779$ [kPa]

$T_{10} = 75.12$ [C]
$p_{10} = 19787$ [kPa]

$QHX_{HTrecup} = 20553$ [kW]

$T_7 = 347.8$ [C]
$p_7 = 19622$ [kPa]

$T_6 = 246.6$ [C]
$p_6 = 19744$ [kPa]

$mdot_{10} = 26.91$ [kg/s]

Gas Turbine

$mdot_{cg1} = 47.13$ [kg/s]

To Stack

Heater   Preheater

HRU = Heat Recovery Unit $Eff_{WHR} = 0.7948$

$Q_{HRU} = 20076$ [kW]
$T_{cg1} = 512$ [C]
$QPrimHx_{actC} = 12160$ [kW]
$dp_{cgPrimHx} = 0.2708$ [kPa]
$NTU_{PrimHx} = 3.391$

$T_{cg2} = 281.7$ [C]
$QPreHtrHxC = 7916$ [kW]
$dp_{cgPreHtr} = 0.1848$ [kPa]
$NTU_{PreHtrHx} = 3.065$

$T_{cg3} = 125.1$ [C]

CO2 Inventory

$massWF_{HP} = 903.7$ [kg]

$massWF_{LP} = 2003$ [kg]

$massWF_{Tot} = 2907$ [kg]

Figure 1 B: Temperature Entropy Plot
Power Cycle for WHR SCO2 System with Titan 130

T-S
Sat Liq
Sat Vap
Heat Source

Net CO2 Efficiency= 22.78%
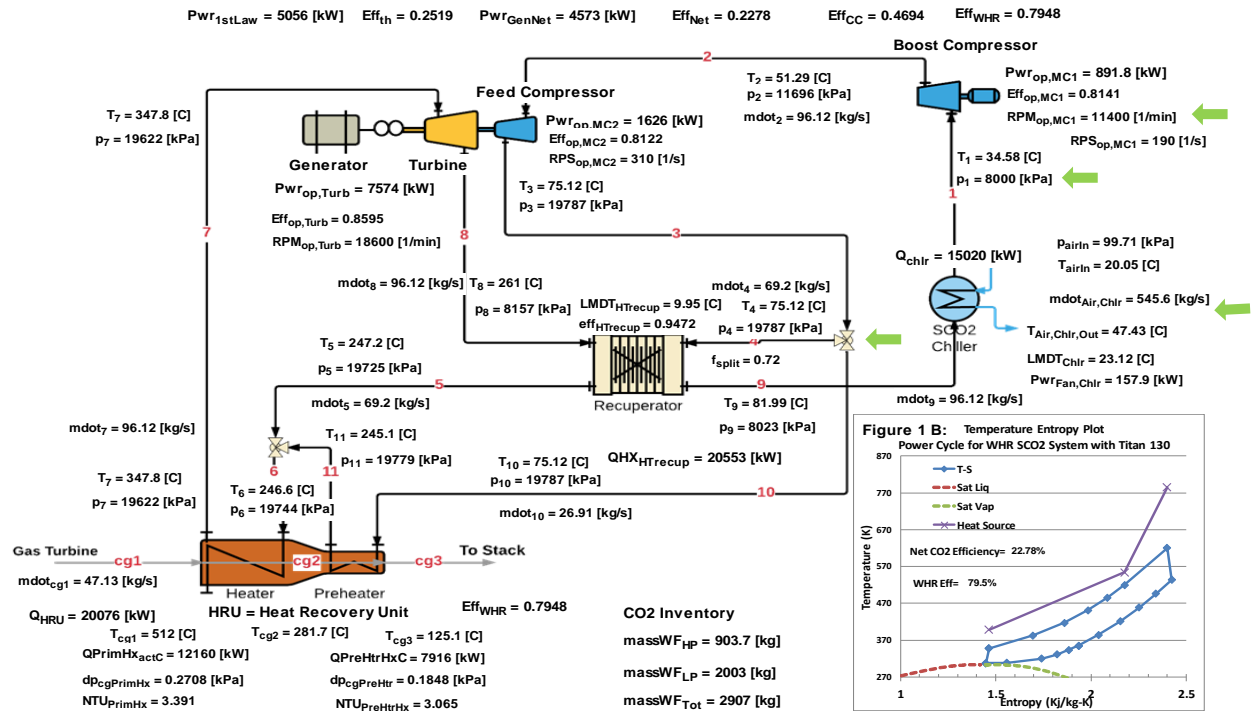
WHR Eff= 79.5%

Temperature (K)

Entropy (Kj/kg-Kj)

Figure 1A & 1B: (1A) Process flow diagram for the 5 MWe sCO₂ Waste Heat Recovery Power Plant. Waste heat is from a Solar Turbine Titan 130. All components use first principles models for the off-design performance. The green arrows indicate primary control variables. (1B) The inserted temperature entropy plot (lower right) shows how the cycle allows the heat source glide temperature to match the CO₂ temperature and thus increase the WHR efficiency.

20MWe
Modular Power Facility

Solar Turbines
A Caterpillar Company

Gas Turbine	15 MWe
sCO2 Plant	5 MWe
Efficiency	47-48%

TITAN 130 GAS TURBINE
MODULAR POWER PLANT

5 MWe sCO2 Bottoming Cycle with
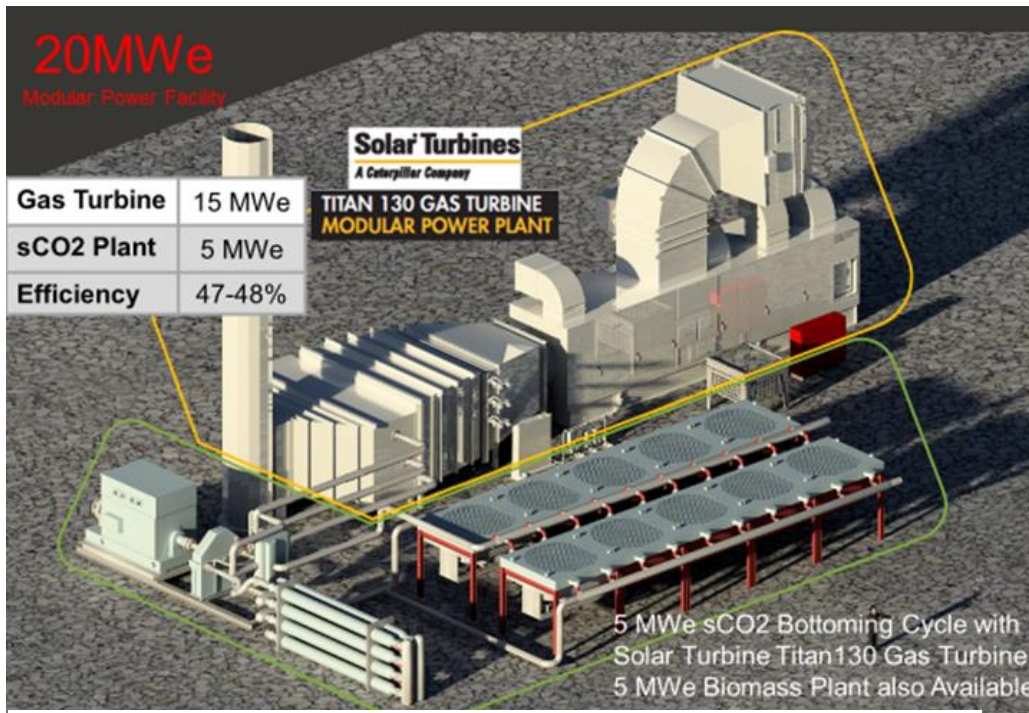Solar Turbine Titan130 Gas Turbine
5 MWe Biomass Plant also Available

Figure 2: Engineering drawing of the sCO2 WHR power plant attached to a Titan 130 gas turbine. The approximate size of the total plant is 60 ft x 90 ft.

1.4 Control Mechanisms

There are four primary control mechanisms within the loop. These are indicated by green arrows in Figure 1.
They consist of controllers to
1. vary the air cooling fan speed (air mass flow rate) to regulate the MC1 compressor inlet temperature,
2. change the boost compressor speed to regulate both the total pressure ratio and sCO_2 mass flow rate,
3. vary the split-flow fraction to regulate the combustion gas exit temperature, to optimize the WHR efficiency,
    and to control the recuperator approach temperature), and
4. control the compressor inlet pressure via inventory control tanks or by using the filling tank reservoir.

This report shows that the combination of these four control mechanisms provides an effective means to mitigate
the effects of increases in ambient heat rejection temperature.

In addition, the plant control system will take advantage of low ambient temperatures to permit condensation
in the air-cooled heat exchanger. This will provide subcooled liquid to the MC1 compressor allowing the power
system to switch from operating in the supercritical mode to operating in the transcritical mode, and thus increase
the amount of power produced by about 0.5 MWe. Compressor inlet guide vanes will likely be required to
accommodate the varying fluid density.   Examples of steady-state off-design performance without condensation
are provided in the subsequent sections to illustrate the expected behavior of the sCO_2 power plant. Off-design
results using condensation are not included in this paper.

2.   sCO₂ WHR Power Cycle Off Design Model

The off-design model uses physical models for all components. Other than pipes, filters, and valves, the major
components consist of heat exchangers and turbomachinery. Brief descriptions of the heat exchanger and
turbomachinery model [3] are provided below in the following paragraphs. The integrated WHR off-design system
was modeled using the Engineering Equation Solver EES64 [4].

2.1 Heat Exchangers Off-Design Models

Four heat exchangers are required for the sCO_2 WHR power system. The sCO_2 gas chiller rejects approximately
15 MWth to the air, the recuperator transfers approximately 20 MWth from the hot leg to the cold leg, and the Heat
Recovery Unit (HRU) transfers about 20 MWth of heat from the combustion gas to the CO_2. The HRU uses two heat
exchangers, the first is a low temperature preheater (about 8 MWth) and the second is a high temperature primary
heat exchanger (about 12 MWth).   More detailed characteristics such as pressure drop, LMDT, and NTU for the
heat exchangers are provided in Figure 1.

One purpose of this off-design development effort was to find appropriate sizes for all the heat exchangers, and
to maximize performance while maintaining acceptable costs. The sizing is especially important for the HRU heat
exchangers as they are the most expensive heat exchangers in the system.

All heat exchanger models use the geometries provided by vendor quotes. The heat exchangers models all used
the effectiveness-NTU method[8] to determine their duty and outlet temperatures given the mass flow rate and the
inlet temperatures and pressures and heat exchanger geometry. Separate stand-alone multi-node models were
first developed, and then correction factors were introduced into the single node models to be used in the off-
design model. The correction factor accounts for LMDT variations along the length of the heat exchanger and
forces the single node heat transfer to equal the multi-node heat transfer.

2.2 Compressor and Turbine Off Design Models

To complete the off-design modeling system it is necessary to have off-design performance maps for the
compressors and turbine. For the conceptual design process, simplified turbomachinery non-dimensional analysis
models are used. These models are based on actual sCO_2 compressor and turbine performance maps as developed
by Barber-Nichols[9] for the Sandia sCO_2 small scale test loops[3]. The simplified models were described by Dyreby [10],
Wright[11] and Fuller et al.[12]. A brief description of the models follows.

2.2.1 COMPRESSOR MODEL

For a pump or compressor, the off-design maps relate the enthalpy change and efficiency to the flow rate through the pump/compressor. The dimensionless forms of these maps plot head coefficient q_{ad} and efficiency as function of the flow rate through the pump/compressor. The dimensionless forms of these maps plot head coefficient q_{ad} and efficiency as function of the flow coefficient (Ø). Curve fits for head coefficient (orange curve) and the efficiency (blue curve) as a function of subscale flow coefficient are shown in Figure 3. They were obtained by fitting the data from the Barber Nichols flow maps for the Sandia small-scale test [14] (operating with a compressor at 50 kW). To use these curves for compressors in the megawatt range (i.e. for the MC1 and MC2 compressor) it is necessary to scale the peak head coefficient to be the design head coefficient of 0.58, and to displace the raw value (or small-scale flow coefficient) from 0.08 to the design flow coefficient of 0.17 as determined from the Ns-Ds design rules (see Balje [13]). The Ns-Ds rules were used to determine a design head coefficient $q_{ad,Design} = 0.58$ and a design flow coefficient $Ø_{Design} = 0.17$ for both the MC1 and MC2 compressors. The peak efficiency was set to 0.82.

Figure 1: Off-design operating characteristics for the turbine. Curves for mass flow rate and efficiency are provided given turbine u/c value.

As used here, the flow coefficient is defined as $Ø = \dot{V}/ND^3$ where $\dot{V}$ is the exit volumetric flow rate, N is the shaft speed (rev/s), and D is the turbine tip diameter. The head coefficient is $q_{ad} = \sqrt{dH_{ad}/u^2}$. In the non-dimensional model used here these curves are not a function of shaft speed in contrast to Dyreby's [10] model.

2.2.2 TURBINE MODEL

For the turbine, the off-design maps relate mass flow rate and isentropic efficiency to the velocity ratio (u/c) at the tip of the turbine. The efficiency curve as a function of u/c is shown as the blue line in Figure 4. The other curve (orange) shows the mass flow rate as a function of u/c. The term u/c is the ratio of the turbine tip speed (u), to c the spouting velocity, $c = \sqrt{2 * dH_{ad}}$. In this equation dH_{ad} is the change in adiabatic enthalpy across the turbine that is a function of inlet and outlet temperature (T) and pressure (p). Because the tip speed is required in the turbine model, it is necessary to know the turbine diameter and shaft speed. These turbine physical properties were determined by selecting the maximum of the turbine efficiency curve to occur at u/c=0.65 and using the Ns-Ds method described in Balje [13].
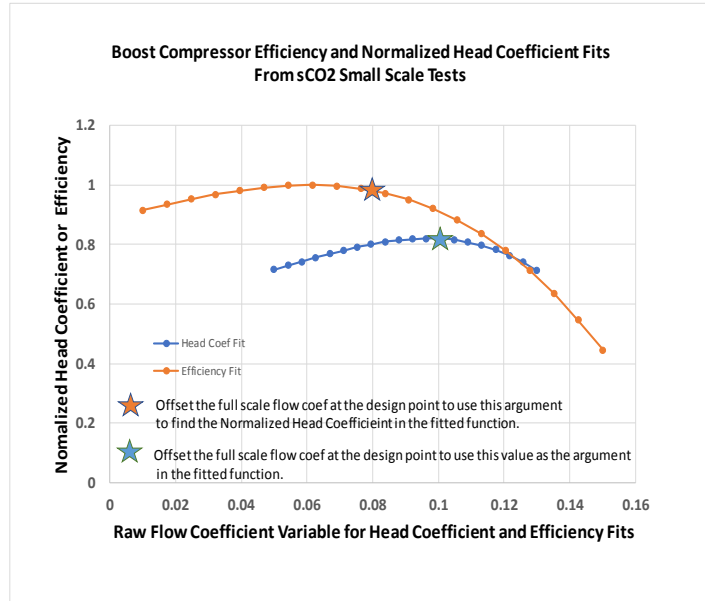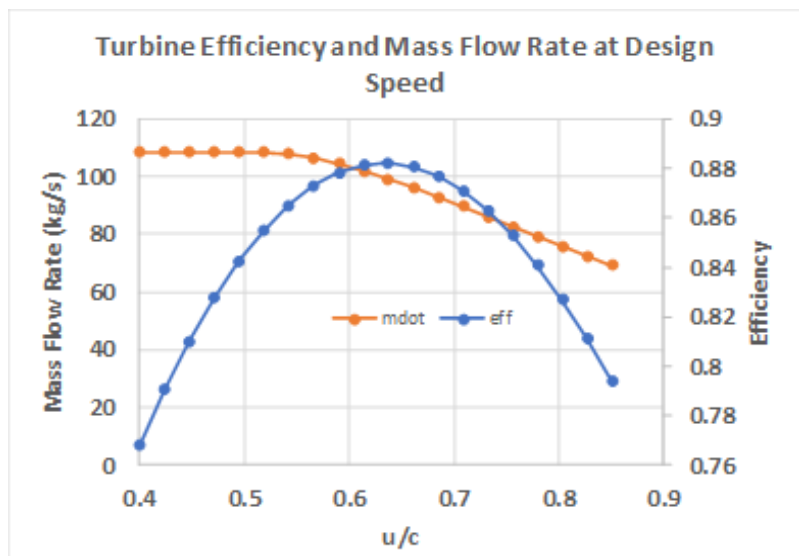

Figure 2: Off-design operating characteristics of the MC1 compressor. Curves for efficiency and normalized head coefficient as a function of flow coefficient.

The EES64 equation solver for the WHR off-design power cycle model then solves for all temperatures, pressures, and flow rate, consistent with the system energy balance and pressure drop and turbomachinery constraints within the loop. The turbomachinery mechanical to electric efficiency is assumed to be 93% (generator, bearing and seal losses).

3. Off-Design Performance

The operating turbomachinery speeds illustrated in Figure 1 are very close to the optimal operating conditions. Because the design conditions were selected to maximize the electrical power, deviations in the control parameters from their design point will generally result in poorer performance, i.e. lower net electrical power. The following paragraphs describe some of the results of the off-design model, by illustrating trends in power generation, state point temperatures, due to changes in the MC1 compressor speed and inlet pressure control variables.

Examples of the off-design performance trends begin by using a constant ambient air temperature (20.04 C). For this ambient temperature, the net generator power and system temperatures are illustrated as a function of changes in the speed control. These results are then followed with a description of the bottoming cycle behavior as a function of ambient air temperature variations (17 C to 38 C) for three different control modes. These results show that the use of the four main control variables can be used to greatly mitigate the degradation in performance due to ambient air temperature increases.

3.1 Electrical Power Versus RPM

The effect of the speed control variable is illustrated in Figure 3. This figure plots Net Generator Power (PwrGenNet) and mass flow rate (mdot) as a function of MC1 rpm, for constant pressure at the inlet to the main compressor, and for constant ambient conditions and air flow. These curves clearly show that the net generator power peaks near the design point rpm (11,400 rpm), and that the mass flow rate increases with increasing rpm. Note that the MC1 speed changes from 9000 rpm to 13200 (a 47% increase), while the net generator power changes by only 135 kW (from 4450 kWe to 4585 kWe, or a 3% change).

3.2 State Point Temperatures Versus RPM

The system temperatures are shown next for the same fixed operating conditions of fixed inlet pressure, ambient temperature, and fixed air flow. Figure 4 plots state point temperatures at each location as a function of rpm. The major trend observed is that all the cold temperatures (1,2,3,9) increase with increasing rpm and that all hot temperatures (11, 5, 8, 7) decrease with increasing rpm. As shown in Figure 3 a higher compressor rpm results in an increase in mass flow rate. Ideally, at constant state point temperatures a larger mass flow rate would always result in higher electrical power generation, but these off-design model results illustrate that in a physical system with waste heat recovery the higher flow rates increase the heat transfer from the hot fluids to the cooler fluids resulting in a decline in the temperature difference between the hot and cold side temperatures. As previously mentioned the net generated power declines the farther away you operate from the design point, due primarily to the efficiency versus u/c curve for the turbine.
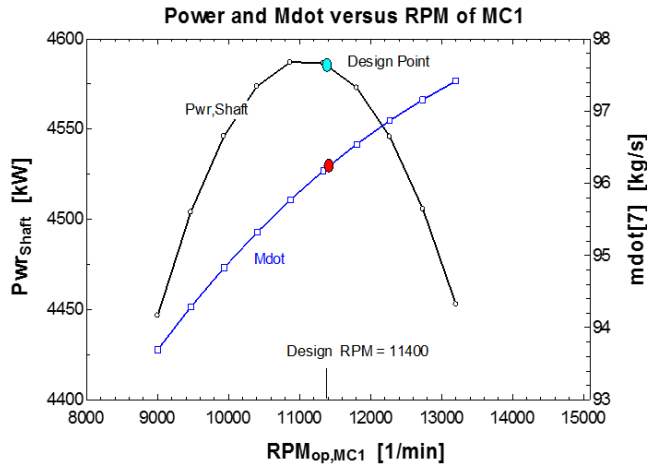
Figure 3: Net power at gen. terminals and mass flow rate versus MC1 rpm.
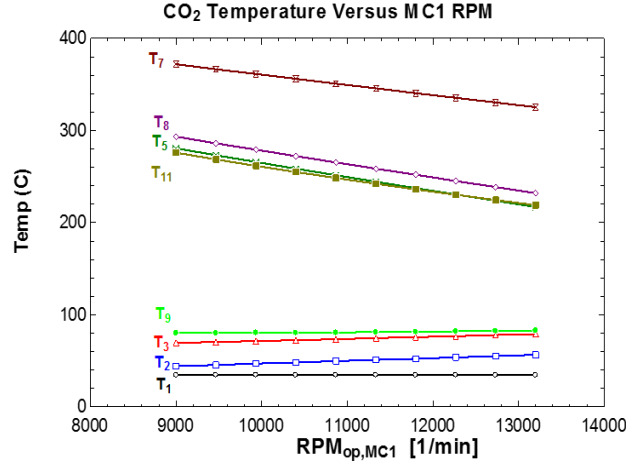

Figure 4: Temperature at node locations as a function of MC1 rpm.

3.3 Off-Design Performance due to Ambient Air Temperature Increases

This section shows how the sCO_2 bottoming cycle responses to ambient air temperature changes. It then shows how air fan speed (air flow rate), MC1 compressor speed, split flow fraction, and control-pressure can be used to mitigate the impact of ambient air temperature increases.

Because the report is focused on the behavior of the sCO_2 power system, the model assumes that the operating parameters (flow rate and combustion gas temperature) of the Titan 130 gas turbine are constant. In fact, gas turbines are very sensitive to ambient air temperature, but this assumption is used to clearly show the impact of ambient temperatures changes on the sCO_2 bottoming cycle behavior. With this assumption, the main results of the off-design sCO_2 bottoming cycle performance are illustrated Figure 5. This figure plots the electrical power at the generator terminals as a function of ambient air temperature for three different operational control cases.

In the first case, the as designed sCO_2 power system is operated at the design conditions and only the ambient air temperature is changed (see blue curve, labeled Pwr Gen DP). All the other variables such as split flow fraction, compressor speed, compressor pressure and fan speed are kept constant. In the second case (green curve) the ambient air temperatures changes but the compressor speed is increased from 11,400 rpm to 16,800, the flow split is decreased from 0.72 to 0.69, and air flow rate is increased from 500 kg/s to 700 kg/s. The inlet pressure is kept constant at 8000 kPa. This figure is labeled Pwr$_{Gen,S}$ and illustrated by

Figure 5: Example illustrating the performance of the sCO2 power plant as a function of ambient inlet air temperature for the design point operating conditions (DP; blue curve). A 2nd case (green curve) that increases the MC1 shaft speed from 11400 to 16800 rpm and with increasing air cooling fan speed (and with minor split flow fraction changes). The 3rd case also increases the compressor inlet pressure.

the olive-green line. The reader can observe that this curve shows a reduction in power as ambient temperature is increased, but the rate of decrease is greatly reduced compared to the baseline case. Finally, the third case (red
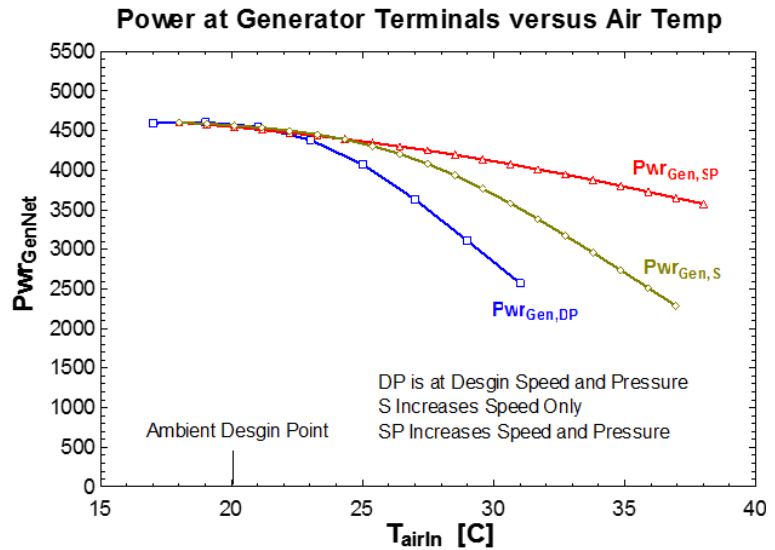
8

curve) is the same as the previous case, but the compressor inlet pressure is also increased. It is increased from 8000 to 9000 kPa and the solver finds a solution up to an ambient temperature range of 38 C, labeled by the red curve (Pwr Gen SP). In this third case, the electrical power reduction due to higher ambient temperature is greatly mitigated. This clearly shows that the proposed control methods (MC1 compressor speed, air fan speed, split flow fraction, and pressure control, when acting in concert can have a major impact on keeping the sCO_2 operating well at elevated ambient temperatures even with dry cooling.

4. Conclusions

The results of off-design performance models for a sCO_2 (supercritical CO_2) waste heat recovery power cycle are presented. The sCO_2 power cycle used split flow with preheating[1] to make effective use of the available exhaust gas heat from a 15 MWe Titan 130 gas turbine. The sCO_2 power cycle uses air cooled heat exchangers, and the plant produces nominally 5 MWe at the generator terminals. Because of the air-cooled heat rejection system, the bottoming cycle is subject to degradation in power product due to increases in ambient air temperature. A unique aspect of the proposed power cycle is the use of a "low-pressure boost compressor" to provide for startup capabilities and to provide a control mechanism to improve off-design behavior due to increases in ambient air temperatures.

The off-design model uses first principle physical models for all the major components. This consists primarily of heat exchanger models and turbomachinery models. The heat exchanger models all use the effectiveness-NTU method. The turbomachinery models use non-dimensional curve fits to sCO2 compressor and turbine designs developed for the Sandia[3] small scale experiments. For the compressor, the models relate compressor efficiency and head coefficient to the flow coefficient. For the turbine, the models relate efficiency and mass flow rate to the velocity ratio u/c.

The paper discusses the primary control mechanisms that include (1) varying the air cooling fan speed, by (2) changing the boost compressor speed, by (3) varying the split-flow fraction, by (4) selecting the compressor inlet pressure. Examples of the system response to these control variables were discussed using plots and curves that showed the net power and the state-point temperatures. The report then demonstrates that the combination of the four control mechanisms provides an effect means to mitigate the effects of increases in ambient heat rejection temperature.

5. Future Work

Dynamic system models for sCO2 power systems are currently being developed and tested using EES64 [4]. These models solve the conservation of mass, momentum and energy equations for all the heat exchangers, pipes, valves, turbines and compressors. The conservation of mass and energy equations are enthalpy based and use the equations defined by Quoilin[15] as used in the Thermocycle Library[16]. The equation of state is tabulated in lookup tables. Only two lookup tables are needed because the heat transfer functions and friction factors are assumed to be a function of mass flow ratio relative to the design point. The two lookup tables provide the enthalpy given the temperature and pressure, or the temperature given the pressure and enthalpy.

The momentum integral form of the momentum equations is used to find the velocity of the CO_2 at all locations. This form of the momentum equation uses the pressure difference between the compressors minus the turbine and minus the pressure drop due to friction in all components as the driving term for a single large slug of CO_2 in the loop as described by Trinh[17] in the TSCYCO code. For the preheating cycle shown in this paper there are about 3-8 tonnes of CO_2 in the loop. Typically, the net driving pressure exceeds the friction by a few 100 kPa, resulting in a time constant of acceleration on the order of 6-15 seconds for most problems. In contrast, the large thermal mass in the piping and heat exchangers results in a thermal response time of about 15-20 minutes. The turbomachinery models use the same non-dimensional equations as described in this report. They are used to provide the pressure changes in the compressors and turbine given the imposed turbomachinery shaft speed (rpm) and the CO2 mass flow rate as derived by the momentum integral equation.

Acknowledgements

References

[1] Campanari S., Lozza G., Macchi E. (1995) "Comparative thermodynamic analysis of ammonia, air and steam cycles for heat recovery from gaseous flows" (in Italian), VIII congress Technologies and Complex Energetic Systems "Sergio Stecco", Bologna, Italy, June 1995.

[2] David Montgomery, Caterpillar ARES Program Manager, "An Otto Rankine Combined Cycle for High Efficiency Distributed Power Generation", https://www.erc.wisc.edu/documents/symp09-Montgomery.pdf, June 10, 2009.

[3] Wright, S. A., Radel, R. F., Vernon, M.E., Rochau, G.E, Pickard, P.S., "Operation and Analysis of a Supercritical CO2 Brayton Cycle", Sandia Report No. SAND2010-0171, 2010.

[4] Klein, S.A., Engineering Equation Solver for Microsoft Windows Operating Systems 64 Bit, Professional Version, F-Chart Software, http://fchart.com, 2016.

[5] Solar Turbines, a Caterpillar Company, https://mysolar.cat.com/en_US/products/power-generation/gas-turbine-packages/titan-130.html, Brochure see modular system, 2017.

[6] Ralph Ordonez, Engine Performance Code Rev. 4.17.1.19.11, SD Natural Gas Engine, TITAN 130-20501S Axial, 60 Hz for location in San Antonio Tx, Jan. 16, 2016.

[7] Steven A. Wright, Chal S. Davidson, William O. Scammell, "Thermo-Economic Analysis of Four Waste Heat Recovery Power Systems", in Proceedings of the ASME paper, 5th International Symposium – Supercritical CO2 Power Cycles, March 2016.

[8] J. P. Holman, "Heat Transfer", Eighth Edition, McGraw Hill, pages 572-590, 1997.

[9] Barber Nichols, http://www.barber-nichols.com/, 2017.

[10] John J. Dyreby, Sanford A. Klein, Gregory F. Nellis, Douglas T. Reindl, "Modeling Off-Design Operation of a Supercritical Carbon Dioxide Brayton Cycle", in Proceedings of Supercritical CO2 Power Cycle Symposium, Boulder, Colorado May 24-25, 2011.

[11] S. A. Wright, A. Z'Graggen, J. Hemrle, "Control of a Supercritical CO2 Electro-Thermal Energy Storage System", Proceedings of ASME Turbo Expo 2013, GT2013-95326, San Antonio, Texas, USA, June 3-7, 2013.

[12] Robert Fuller, et. Al., "Turbomachinery for a Supercritical CO2 Electro-Thermal Energy Storage System", in Proceedings of the ASME Turbo Expo 2013, GT2013-95112 San Antonio Texas, June 3-7, 2013.

[13] O.E. Balje, "Turbomachines: A guide to Design, Selection and Theory", John Wiley and Sons, 1981.

[14] Thomas Conboy, S. Wright, et.al., "Performance Characteristics of an Operating Supercritical CO2 Brayton Cycle", in Proceedings of the ASME Turbo Expo 2012, GT2012-68415, Copenhagen, Denmark, June 11-15, 2012.

[15] Quoilin Sylvain, Desideri A., Wronski J., Bell Ian, Lemort V., "ThermoCycle: A Modelica library for the simulation of thermodynamic systems", Proceedings of the 10th International Modelica Conference, Lund Sweden, March 10-12, 2014.

[16] Quoilin Sylvain, et al., ThermoCycle: http://www.thermocycle.net/, January 2018.

[17] Trinh Tri Q., "Dynamic Response of the Supercritical CO2 Brayton Recompression Cycle to Various System Transients", Master of Science in Nuclear Science and Engineering, Massachusetts Institute of Technology, August 2009.